Bio-Medical Applications

Eur. Phys. J. Special Topics **143**, 89–94 (2007)

DOI: 10.1140/epjst/e2007-00075-1

THE EUROPEAN PHYSICAL JOURNAL SPECIAL TOPICS

Macroscopic dynamics of cancer growth

S.A. Menchón[1] and C.A. Condat[1]

[1]CONICET and FaMAF, Universidad Nacional de Córdoba, 5000-Córdoba, Argentina

Abstract. Macroscopic modeling is used to describe various aspects of cancer growth. A recently proposed "dysnamical exponent" hypothesis is critically examined in the context of the angiogenic development. It is also shown that the emergence of necroses facilitates the growth of avascular tumors; the model yields an excellent fit to available experimental data, allowing for the determination of growth parameters. Finally, the global effects of an applied antitumoral immunotherapy are investigated. It is shown that, in the long run, the application of a therapeutical course leads to bigger tumors by weakening the intraspecific competition between surviving viable cancer cells. The strength of this model lies in its simplicity and in the amount of information that can be gleaned using only very general ideas.

1 Introduction

Cancer growth is unique in its complexity and enormously challenging in its diversity. Mathematical modeling has helped us to understand the growth dynamics and to formulate the right questions about the relevant mechanisms [1]. Taking advantage of the advent of powerful computers, a host of *mesoscopic* models have been developed to descrsibe various aspects of the disease [2–5]. A limitation of the mesoscopic approach is that it is largely based on results obtained by performing simulations that require specific parameter values. It is therefore useful to complement this type of modeling with a more general approach that, while forgoing a detailed description of cancer growth, captures its most relevant elements. This can be done by using a *macroscopic* scheme, in which the tumor is considered as a single entity whose behavior can be predicted in terms of a few characteristic parameters and of its global interaction with the environment. The realization [6] that the ontogenetic growth model of West, Brown and Enquist (WBE) [7] could be used to describe the global properties of cancer growth gave new life to macroscopic modeling. The use of WBE-like modeling has proved fruitful, leading to the description of multicellular tumor spheroid (MTS) growth under conditions of stress and underfeeding [8], to the understanding of the effect of necroses on the spheroid growth rate [9], and to discussions on the effect of tumor stage changes on growth rates [10]. A few processes are crucial to determine or modify the tumor growth rate. In this paper we will apply this technique to analyze three of them: the emergence of angiogenesis, which changes the nutrient distribution pattern, the onset of necrosis, which decreases the number of cancer cells that need to be fed, and the application of a therapeutic course that destroys a large number of cancer cells.

2 Basic model

We start by writing down the law of conservation of energy. We do this following Ref. [7]: if B is the energy income rate to all of the organism's cells, the increment ΔN in the total number

of live cancer cells during a time interval Δt is given by the equation,

$$B\Delta t = N\beta\Delta t + \varepsilon\Delta N, \tag{2.1}$$

where β is the single cell metabolic rate and ε is the average energy necessary to create a single cell. Defining $b = \beta/\varepsilon$ and writing the organism mass as $m = Nm_c$, where m_c is the average mass of a single cell, we can transform Eq. 2.1 into a differential equation,

$$\frac{dm}{dt} = \frac{m_c}{\varepsilon}B(m) - bm. \tag{2.2}$$

Here we must model the basal metabolic rate $B(m)$. It seems reasonable to assume that different stages of cancer are characterized by different forms for the metabolic rate $B(m)$. Delsanto and co-workers [8] suggested that $B(m) = B_0 m^p$, with $p\epsilon(0,1)$. This would include the cases of diffusion-controlled feeding ($p = 2/3$) and of a well-developed fractal network ($p = 3/4$). The first would correspond to avascular in vivo tumors and MTSs, while the latter would correspond to the fully developed vascular stage. Using this power-law form for $B(m)$, the solution to Eq. 2.2 is,

$$m(t) = M\left\{1 - \left[1 - \left(\frac{m_0}{M}\right)^{1-p}\right]\exp^{-(1-p)bt}\right\}^{1/(1-p)}, \tag{2.3}$$

where m_0 is the initial mass and M is the asymptotic tumor mass,

$$M = \left(\frac{a}{b}\right)^{1/(1-p)}, \tag{2.4}$$

with $a = m_c B_0/\varepsilon$.

3 Angiogenesis

Angiogenesis is the growth of the vascular system feeding the tumor. Although several models for angiogenesis have been developed in the past [11,12], interest in this process has been rekindled by the development of antiangiogenic drugs, which could serve as effective anticancer weapons [13]. Guiot and coworkers [10] used the concept of dynamic exponent to explore the influence of the development of neoplastic vasculature. They conjectured that the exponent p increases when the dominant nutrient-replenishment mechanism switches from passive diffusion to active angiogenesis-mediated perfusion. Comparison with experiments in tumor implanted in mice indicated that, independently of the cancer type, p increases above $3/4$ after a few weeks. It was suggested that values of p larger than $3/4$ may indicate that active diffusion "... is complemented by other supply mechanisms, such as passive diffusion, when vascular density approaches its plateau".

In our opinion, we cannot describe two different mechanisms using a single power-law term. In fact, after the onset of angiogenesis, two feeding channels coexist, each channel contributing a different term to the metabolic rate. Passive diffusion is represented by a term with the $2/3$ exponent, while neovascularization requires a new term, whose exponent evolves following the angiogenetic development. Therefore, we propose to represent the metabolic rate as,

$$B(m) = B_{01}m^{2/3} + B_{02}(m)m^p. \tag{3.1}$$

Both p and the coefficient B_{02} depend on the vascularization stage and, therefore on the instantaneous tumor mass. Since vascularization evolves gradually, the exponent p would evolve continuously until it reaches the value $p = 3/4$, which corresponds to fully developed angiogenesis. B_{02}, on the other hand, is initially equal to zero and grows monotonically until it reaches the saturation value corresponding to full-blown angiogenesis. It is therefore reasonable to suggest that, while the vascular net is emerging, the product $B_{02}(m)m^p$ may grow approximately as a power higher than $3/4$. In the case of fully vascularized in vivo tumors, the second term in Eq. 3.1 will dominate, nutrient diffusion being only a minor, residual mechanism.

The use of an antiangiogenic therapy would either inhibit the formation of new blood vessels or weaken and destroy those already in place. In contrast with conventional chemotherapy, it would not directly shrink m, but it would decrease the second term on the right-hand side of Eq. 3.1, leading to a reversal or at least a slowing down of growth. It has been observed that antiangiogenic therapies work best when used in combination with cytotoxic drugs [13]. We believe that macroscopic modelling can be used to suggest ways to optimize the combined therapy and to understand why it works.

4 Necrosis

We have recently shown that the usual assumption that the basal metabolic rate depends on the individual mass following a power law is invalidated by the emergence of necroses [9]. In the case of MTSs, the nutrients arrive at the cells by diffusion alone and $p = 2/3$. MTSs are experimental systems widely used to model many aspects of cancer growth and therapy [14]. Those MTS whose diameters exceed about 0.7 mm develop a necrotic core, because oxygen and nutrients cannot penetrate beyond a viable outer layer. After the onset of necrosis, growth continues, but the viable layer thickness Δ stays approximately constant [14], a result already predicted by Burton in the 60's [15]. *Type I* spheroids do not develop necroses, reaching a maximum radius

$$R^I = (3/4\pi\rho)^{1/3}\,(a/b), \tag{4.1}$$

where ρ is the mass density. *Type II* spheroids are those that develop a necrotic core. For these spheroids two well-defined growth regimes are observed. At the beginning, they follow the $p = 2/3$ law, but at times later than a transition time τ defined by $m(\tau) = \hat{m} \equiv (4/3)\pi\rho\Delta^3$, the live cell mass is related to the spheroid radius r through the equation $m(t > \tau) = \rho V_c$, where V_c is the volume occupied by live cells. It is not difficult to see that the live cell mass evolves according to the equations [9],

$$\frac{dm}{dt} = \begin{cases} am^{2/3} - bm & \text{if } m < \hat{m} \\ \dfrac{a\hat{m}^{2/3}}{12}\left[\left(4\dfrac{m}{\hat{m}} - 1\right)^{1/2} + \sqrt{3}\right]^2 - bm & \text{if } m > \hat{m} \end{cases} \tag{4.2}$$

The spheroid evolution at times $t > \tau$ depends on the relative sizes of M and $\hat{m}$.

a) If $\hat{m} < (1/27)(a/b)^3 = (1/27)M$, the viable shell is very thin and growth is unbounded.
b) If $(1/27)M < \hat{m} < M$, the viable cell mass grows monotonically until it reaches its steady state value,

$$m_s^{II} = \frac{3\hat{m}}{2\,(1-3Q)^2}\left(\frac{2}{3} + Q + Q\sqrt{\frac{4}{Q} - 3}\right), \tag{4.3}$$

where $Q = (\hat{m}/M)^{1/3} \leq 1$. The steady-state mass grows from $m_s^{II} = \hat{m}$ when $Q = 1$ up to $m_s^{II} = \infty$ when $Q \to (1/3)^+$.
c) If $M < \hat{m}$, there is no necrosis and the steady state is given by $m_s^I = (a/b)^3$.

Very recently, Guiot and co-workers [10] indicated that experimental growth data on implated spheroids reported by Steel [16] could be fitted by the solution to Eq. 4.2 provided a "dynamic" p was used. In Fig. 1 we show that an almost perfect fit can be achieved if we assumed instead that a necrotic core emerges. The final mass for this implanted spheroid would be $M = 0.683$ g if there were no necrosis. Because of the emergence of the necrotic core, Eq. 4.3 indicates that the final mass is $m_s^{II} = 2.49$ g, almost four times as large.

As it is clear from Fig. 1, the emergence of a necrosis helps the implanted tumor to reach larger sizes. This is achieved by concentrating resources on the viable outer layer. This phenomenon occurs also in solid *in vivo* tumors. In Ref. [9] we gave a prescription to use experimental MTS data to obtain the values of the parameters a and b that characterize different cancer cell lines. The availability of such values would help us to set constraints on growth models.

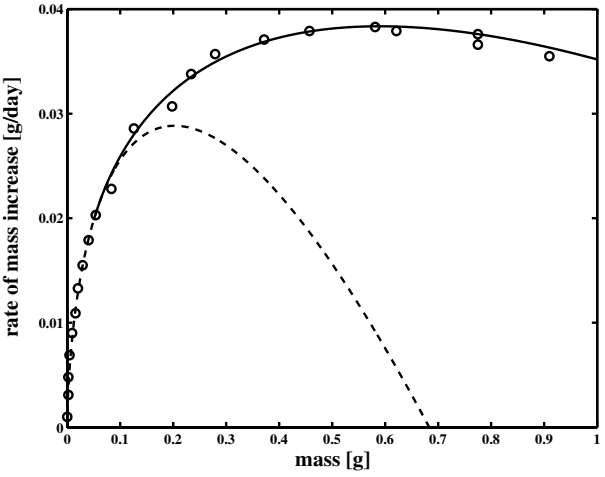

Fig. 1. Plot of dm/dt vs m. The fitting lines (dashed for $m < \hat{m}$ and solid for $m > \hat{m}$) agree precisely with the experimental data reported by [10] (dots). In the absence of necrosis, the spheroid would have evolved following the dashed line. Parameter values are $\hat{m} = 0.05\,\mathrm{g}$, $a = 0.251\,\mathrm{g}^{1/3}/\mathrm{day}$, and $b = 0.285/\mathrm{day}$.

5 Immunotherapy

Most therapeutical procedures involve the direct destruction of cancer cells. Unless the nutrient distribution channels are also affected as it (notably) occurs with antiangiogenic therapies, the killing of active cancer cells involves the local availability of additional nutrients to the remaining cancer cells. After a recovery time has elapsed, the surviving cancer cells can take advantage of the nutrient availability to start faster reproduction. We have seen this effect clearly in a mesoscopic model for cancer immunotherapy [17]. In this type of therapy, the immune response is boosted, by the use of cytokines, for instance [18,19]. Cytotoxic lymphocytes are thus induced to attack cancer cells. Researchers are currently trying to find ways to optimize the immune response in order to control tumor growth [17,20]. Next we use macroscopic modeling to investigate the global effects of the application of immune therapy to a neoplasm. For simplicity, we assume a multicellular spheroid without necrotic core which is supplied by diffusive nutrient distribution, although the results should be qualitatively valid in general.

We assume that immunotherapy kills a fraction D of those cancer cells located at a distance less than δ from the tumor boundary. Under these conditions, it is convenient to write the Eq. 2.2 as a function of the volume:

$$\frac{dv}{dt} = a_v v^{2/3} - bv, \tag{5.1}$$

where $a_v = a\rho^{-1/3}$ and ρ is the density. At time $t = t_0$, when the tumor radius is r_0 and its volume is $v_0 = 4\pi r_0^3/3$, a therapeutic dose is applied and $D\rho v_s/m_c$ cells die ($D \leq 1$). The volume v_s of the spherical shell that is effectively affected by the therapy is given by,

$$v_s = (36\pi)^{1/3}\delta v_0^{2/3} - (4\sqrt{3}\pi)^{2/3}\delta^2 v_0^{1/3} + \frac{4\pi}{3}\delta^3, \tag{5.2}$$

if $r_0 > \delta$, and $v_s = v_0$ if $r_0 \leq \delta$. For $t \geq t_0$, we have:

$$\frac{dv}{dt} = a_v v^{2/3} - b(v - Dv_s), \tag{5.3}$$

The steady state is given by the following equation:

$$a_v v^{2/3} - bv + bDv_s = 0. \tag{5.4}$$

It is obvious that the volume v_{eq} of the new equilibrium state is greater than $(a_v/b)^3$. In Fig. 2 we can see how v_{eq} increases as a function of the volume v_0 of the tumor at the time of

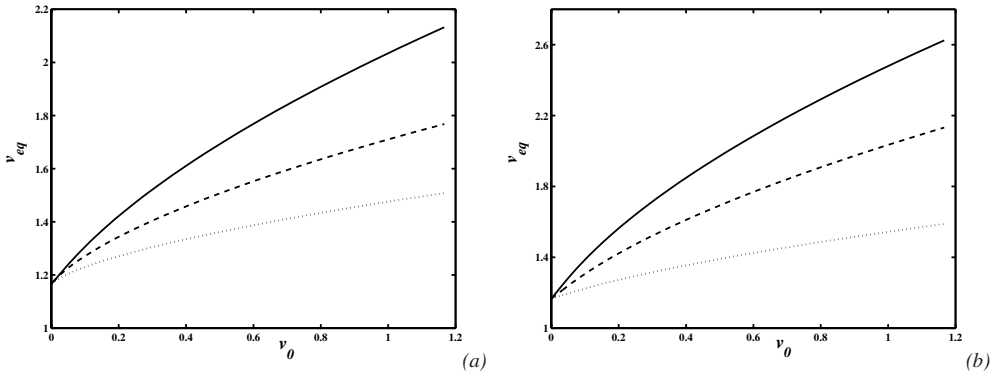

Fig. 2. Post-therapy equilibrium value v_{eq} as a function of the volume at which immunotherapy is applied. We have chosen $a_v = 0.3\,\mathrm{cm/day}$ and $b = 0.285/\mathrm{day}$. (a) Destruction of a fraction $D = 0.5$ of the viable cells in an outer layer whose thickness is $\delta = 0.05\,\mathrm{cm}$ (dash-dotted), $0.1\,\mathrm{cm}$ (dashed) and $0.2\,\mathrm{cm}$ (solid). (b) Destruction of a fraction $D = 0.2$ (dash-dotted), 0.5 (dashed) and 0.8 (solid) of the viable cells in an outer shell of thickness $\delta = 0.2\,\mathrm{cm}$.

the therapy, for different values of δ and D. This increase was to be expected. What may come as a surprise is the realization that the most efficient the therapy is in eliminating cancer cells, the stronger is the cancer cell repopulation process. This effect is clearly seen in a mesoscopic model of immunotherapy, and is independent of the tumor shape [17].

To conclude, we would like to underline the importance of connecting the macroscopic and mesoscopic approaches. This has already been done for MTSs via the introduction of an intermediate model that permits us to relate the characteristic parameters of these two formulations [21], but more work remains to be done.

This work was supported by CONICET, through PIP 6311/05 grant, and by SECyT-UNC.

References

1. For a lucid introduction see N.F. Britton, *Essential Mathematical Biology* (Springer, London, 2003)
2. M. Scalerandi, A. Romano, G.P. Pescarmona, P.P. Delsanto, C.A. Condat, Phys. Rev. E **59**, 2206 (1999)
3. M. Scalerandi, B. Capogrosso Sansone, C. Benati, C.A. Condat, Phys. Rev. E **65**, 051908 (2002)
4. S.C. Ferreira Jr., M.L. Martins, M.J. Vilela, Phys. Rev. E **67**, 051914 (2003)
5. Yi Jiang, J. Pjesivac-Grbovic, Ch. Cantrell, J.P. Freyer, Biophs. J. **89**, 3884 (2005)
6. C. Guiot, P.G. Degiorgis, P.P. Delsanto, P. Gabriele, T.S. Deisboeck, J. Theor. Biol. **225**, 147 (2003)
7. G.B. West, J.H. Brown, B.J. Enquist, Nature **413**, 628 (2001)
8. P.P. Delsanto, C. Guiot, P.G. Degiorgis, C.A. Condat, Y. Mansury, T.S. Deisboeck, Appl. Phys. Lett. **85**, 4225 (2004)
9. C.A. Condat, S.A. Menchón, Physica A **371**, 76 (2006)
10. C. Guiot et al., J. Theor. Biol. **240**, 459 (2006)
11. M.J. Holmes, B.D. Sleeman, J. Theor. Biol. **202**, 95 (2000)
12. B. Capogrosso Sansone, M. Scalerandi, C.A. Condat, Phys. Rev. Lett. **87**, 128102 (2001)
13. R.S. Kerbel, Science **312**, 1171 (2006)
14. W. Mueller-Klieser, Crit. Rev. Oncol./Hematol. **36**, 123 (2000)
15. A.C. Burton, Growth **30**, 159 (1966)
16. G.G. Steel, *Growth Kinetics of Tumours* (Oxford, Clarendon Press, Oxford, 1977)
17. R. Ramos, C.A. Condat, unpublished; G. Rivera, M.S. thesis. Univ. of Puerto Rico, Mayagüez, PR (2005)
18. D. Kirschner, J.C. Panetta, J. Math. Biol. **37**, 235 (1998)

19. O. Sotolongo-Costa, L. Morales Molina, D. Rodríguez Pérez, J.C. Antoranz, M. Chacón Reyes, Physica D **178**, 242 (2003)
20. See, for example, A.M. Hicks et al., Proc. Nat. Acad. Sci. (USA) **103**, 7753 (2006)
21. P.P. Delsanto, M. Griffa, C.A. Condat, S. Delsanto, L. Morra, Phys. Rev. Lett. **94**, 148105 (2005)